Kinase Activity Assays

Deutsche Ausgabe: DOI: 10.1002/ange.201507580
Internationale Ausgabe: DOI: 10.1002/anie.201507580

Rare Earth Ion Mediated Fluorescence Accumulation on a Single Microbead: An Ultrasensitive Strategy for the Detection of Protein Kinase Activity at the Single-Cell Level

Xiaobo Zhang, Chenghui Liu, Honghong Wang, Hui Wang, and Zhengping Li**

Abstract: *A single microbead-based fluorescence imaging (SBFI) strategy that enables detection of protein kinase activity from single cell lysates is reported. We systematically investigated the ability of various rare earth (RE) ions, immobilized on the microbead, for specific capturing of kinase-induced phosphopeptides, and Dy^{3+} was found to be the most prominent one. Through the efficient concentration of kinase-induced fluorescent phosphopeptides on a Dy^{3+}-functionalized single microbead, kinase activity can be detected and quantified by reading the fluorescence on the microbead with a confocal fluorescence microscope. Owing to the extremely specific recognition of Dy^{3+} towards phosphopeptides and the highly-concentrated fluorescence accumulation on only one microbead, ultrahigh sensitivity has been achieved for the SBFI strategy which allows direct kinase analysis at the single-cell level.*

Protein phosphorylation catalyzed by protein kinases (PKs) is the most frequent post-translational modification (PTM), and phosphorylation plays critical regulatory roles in most fundamental metabolic and cell-signaling processes.[1] Increasing evidence has demonstrated that aberrant PK activities may lead to various human diseases, including cancers.[2] Therefore, PKs have attracted great attention because their aberrant activities may serve as biomarkers for a variety of human diseases. More importantly, PKs have been recognized as an important family of molecular targets for the development of new kinase inhibitor drugs in regard to cancer treatments.[3] Thus, accurate detection of PK activities is of great significance for fundamental biological research, clinical diagnosis, and drug discovery. PK activities, along with other protein levels, can be stochastic and often show non-genetic cell-to-cell variations. Many cancers, including aberrant kinase activity-associated ones, may typically begin with cellular abnormalities in a small minority of cells, especially at their early stages.[4] Therefore, the accurate measurement of PK activities at the single-cell level may provide information critical to understanding PK-related disease initiation, progression, as well as the therapeutic responses.[5]

Numerous methods have been established for the detection of PK activities,[6] which have been well summarized in recent reviews.[6n,o] Although these existing assays have made great advances for assessing PK activities, most of them can only measure the population-averaged result of kinase activities in large numbers of cells owing to sensitivity limitations, which may mask the differences of PK activities among individual cells. There are only a few reports that are capable of assaying kinase activities in single cells.[5] Unfortunately, these single cell detection systems are resource-intensive and elaborately designed, requiring specialized skills in either microfluidic processing or instrument modification, and thus limiting their wide applications in ordinary labs. Therefore, simple, versatile, and reliable method for measurements of PK activities at the single-cell level is still urgently desired.

Because PK analysis lacks a generic amplification step, such as during nucleic acid replication, highly selective and efficient enrichment of PK-produced phosphopeptides on certain solid matrix is considered to be a powerful way to improve the detection sensitivity. Herein, by using protein kinase A (PKA) as a proof-of-concept target, we developed a robust single microbead-based fluorescence imaging (SBFI) strategy which allows the accurate detection of PKA activity at the single-cell level. Traditional bead-based bioassays coupled with fluorescence enrichment are generally conducted with numerous beads in one reaction.[7] As a result, the fluorescence signal accumulated on each individual bead is greatly diluted. When the concentration of target molecules is ultralow, only a small minority of beads can generate target-responsive fluorescence signal, which will be hidden in the average of bulk measurements. In contrast, for the SBFI strategy, a single microbead is the ultimate reactor for enriching fluorescence signals, so the fluorescence of the microbead as well as the resulted detection sensitivity can be significantly enhanced because the same amount of fluorophores will be highly concentrated on a single bead rather than dispersed on numerous beads.

On the other hand, another key feature of the SBFI strategy is the highly specific recognition of phospho-affinity materials functionalized on the microbead to differentiate the kinase-induced fluorescent phosphopeptides from a large pool of nonphosphorylated peptide substrates. Several transition metal ions (for example, Zr^{4+}, Ga^{3+}, or Ti^{4+}) are traditionally used as phospho-affinity materials to recognize PK-induced phosphopeptides.[6g,i,j,7c,8] These existing metal ion-based affinity assays typically suffer from nonspecific

[*] X. Zhang, Prof. Dr. C. Liu, H. Wang, H. Wang, Prof. Dr. Z. Li
Key Laboratory of Applied Surface and Colloid Chemistry
Ministry of Education, Key Laboratory of Analytical
Chemistry for Life Science of Shaanxi Province
School of Chemistry and Chemical Engineering
Shaanxi Normal University
Xi'an 710062, Shaanxi Province (P.R. China)
E-mail: liuch@snnu.edu.cn
lzpbd@snnu.edu.cn

Supporting information for this article is available on the WWW under http://dx.doi.org/10.1002/anie.201507580.

binding of nonphosphorylated peptides, especially peptides containing acidic residues,[7c,9] which makes it difficult to discern the small fraction of phosphopeptides produced by low abundance PKs. We recently found that rare earth (RE) ions may potentially serve as excellent candidates for selectively recognizing phosphorylated peptides.[10] RE ions are hard Lewis acids and prefer to bind negatively charged phosphate groups than acidic peptide residues,[11] which is beneficial to suppress the nonspecific adsorption of nonphosphorylated peptides. The trivalent RE ions also have abundant f-orbitals which expand the coordination sites to bind six to twelve ligands to one single metal ion.[9a,12] These facts give us a clear indication that certain RE ions may serve as new ideal choices in phospho-affinity materials. Unfortunately, there have been no systematical studies on the binding abilities of different RE ions towards phosphopeptides. In this work, we systematically investigated the binding affinity of various RE ions with PKA-produced phosphopeptide substrates by fluorescence imaging. Eventually, Dy^{3+} was found to be the best choice. By using a Dy^{3+}-functionalized single microbead (Dy-MB) as the matrix for highly specific and efficient concentration of PKA-induced fluorescent phosphopeptides, single-cell sensitivity was achieved for the detection of PKA activity.

Figure 1 illustrates our proposed strategy for RE ion screening (by using multiple microbeads), as well as for the detection of PKA activity (by using a single microbead). Streptavidin (STV)-modified magnetic sepharose microbeads (STV-MBs) are used as the carrier for RE ions loading and phosphopeptide enrichment. A 5′-phosphorylated and 3′-biotinylated single-stranded DNA (ssDNA; PO_4-T25-Biotin) is first immobilized on the MBs through the STV-biotin interaction. RE ions can readily bind with the ssDNA on the bead surface through both the phosphate backbone and particularly through the 5′-terminal phosphate group of ssDNA.[13] After strong binding with the ssDNA, the RE ions still have free coordination sites because they can offer up to twelve coordination sites,[9a] which may further capture PKA-induced phosphopeptides. To evaluate the binding affinity of different RE ions towards the phosphopeptides, different types of RE ion-functionalized MBs (RE-MBs) were respectively incubated with the TAMRA-peptide substrate treated with 50 μU μL^{-1} (microunits per μL) of PKA or in the absence of PKA (blank). The RE-MBs were then isolated and immediately subjected to fluorescence imaging.

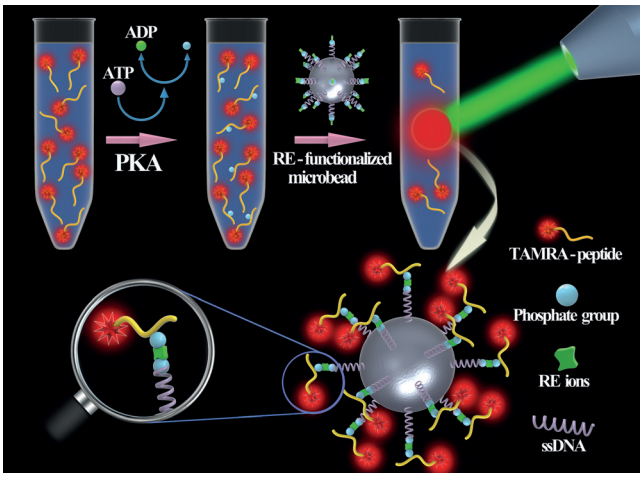

Figure 1. Illustration of RE-functionalized microbeads for capturing PKA-induced phosphopeptides, as well as for the detection of PKA activity. In the presence of PKA, the γ-phosphoryl of ATP can be transferred to the hydroxy group of serine in the TAMRA-LRRASLG substrate, making a portion of the TAMRA-peptides phosphorylated. These phosphorylated TAMRA-peptides can be captured rapidly by the RE-MB while the nonphosphorylated ones will not, which make the microbead highly fluoresce around the bead surface under laser irradiation. PKA activity can be quantitatively reflected by the fluorescence signal of the RE-MB. The RE-MBs are prepared by first immobilizing biotinylated ssDNA molecules (PO_4-T25-Biotin) on the STV-MBs and then coordinating RE ions by the ssDNA.

Representative fluorescence images of these RE-MBs under the same imaging conditions are shown in the Supporting Information (Figure S1). The RE ions can be classified into three groups. For the light lanthanide ions (La^{3+} to Nd^{3+}), the fluorescence responses of the RE-MBs incubated with the PKA-treated samples and the blank (without PKA) are both very low, indicating that under our experimental conditions, the binding ability of these RE ions for phospho-containing biomolecules are relatively weak. Interestingly, most of the middle lanthanides (Sm^{3+} to Dy^{3+}) plus Y^{3+}, particularly Dy^{3+}, appear to favor strong interaction with the PKA-induced phosphopeptides. More importantly, this group of RE ions also exhibits negligible adsorption of nonphosphorylated peptide substrates. In contrast, although the heavy lanthanide ions (Ho^{3+} to Lu^{3+}) show strong binding preference for the PKA-induced phosphopeptides, the nonspecific adsorption of the nonphosphorylated TAMRA-peptide also shows a remarkably increasing tendency with the increase of atomic number from Ho^{3+} to Lu^{3+}. The high signal-to-blank (S/B) ratio may lead to high sensitivity, especially for the detection of PKA at very low abundances. As can be seen from Figure 2, the best S/B ratio is obtained by using Dy^{3+} as the affinity element, indicating that Dy^{3+} is an ideal choice for PKA analysis owing to its highly specific binding of PKA-induced phosphopeptides and almost no nonspecific binding of the nonphosphorylated ones.

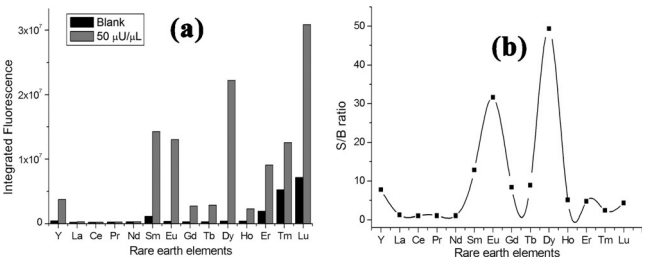

Figure 2. a) Fluorescence responses of different RE-MBs after incubation with the TAMRA-LRRASLG substrate treated with 50 μU μL^{-1} PKA and in the absence of PKA (blank); b) the corresponding signal-to-blank (S/B) ratios of different RE-MBs.

Using Dy^{3+} as the phospho-affinity element, the results displayed in Figure 3 demonstrate the significant advantage of the single Dy-MB-based SBFI strategy over the multiple

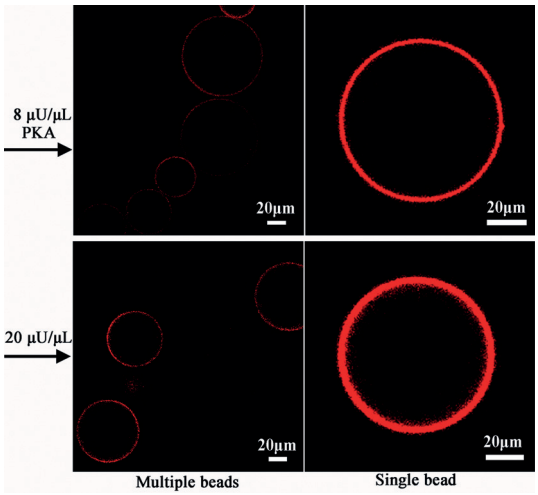

Figure 3. The fluorescence imaging results by using multiple Dy-MBs and a single Dy-MB for the detection of the same concentrations of PKA. The multiple Dy-MBs and the single Dy-MB were incubated with the same PKA reaction mixtures for both 1 hour, respectively. It should be noted that the fluorescence signals of all the corresponding blank controls for both the multiple Dy-MBs and single Dy-MB are negligible in this study (data not shown). PMT HV for imaging = 650 V.

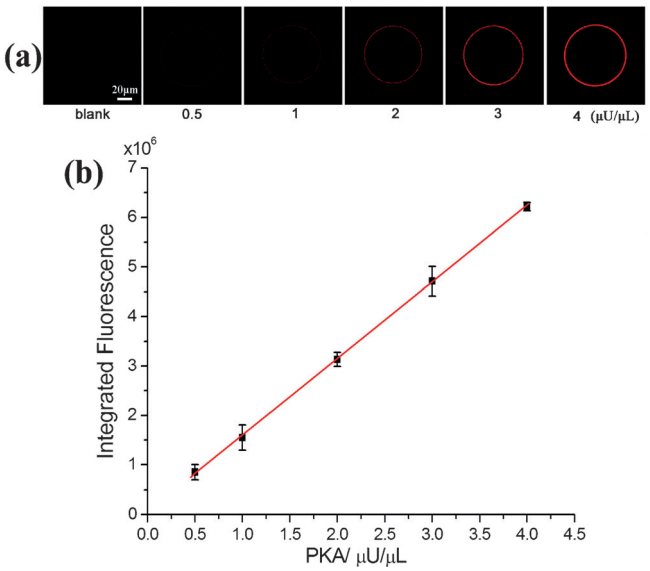

Figure 4. a) Fluorescence images of the Dy-MBs treated with ascending PKA activities from 0 (blank) to 4 $\mu U\,\mu L^{-1}$ (PMT HV = 650 V); b) the relationship between the integrated fluorescence signals of the Dy-MB and the PKA activity. Error bars represent the standard deviation from three independent measurements.

MBs-based assay for the detection of PKA activity at low PKA concentrations. In this study, the multiple Dy-MBs ($\sim 1\,mg\,mL^{-1}$) and the single Dy-MB are incubated respectively with the same PKA reaction mixtures for 1 hour. In such cases, the mixtures for both the multiple Dy-MBs and the single Dy-MB contain the same amount of PKA-induced fluorescent phosphopeptides. For the sample containing the multiple Dy-MBs, the fluorescent phosphopeptides will be dispersed onto the surface of different beads, making the fluorescence signal per bead greatly diluted. In contrast, for the single Dy-MB sample, the same amount of fluorescent phosphopeptides will be highly concentrated on only one bead, rendering the fluorescence signal of the single Dy-MB significantly enhanced. As can be seen from Figure 3 that both 8 $\mu U\,\mu L^{-1}$ and 20 $\mu U\,\mu L^{-1}$ PKA-induced fluorescence responses of the single Dy-MB are strikingly enhanced compared with those by using multiple Dy-MBs. In this regard, by integration of the distinct advantages of Dy^{3+} for highly selective recognition of kinase-induced phosphopeptides and a single microbead as the ultimate assay unit for highly-concentrated fluorescence enrichment, a Dy^{3+}-assisted SBFI strategy can be established for ultrasensitive detection of protein kinase activities.

The analytical performance of the proposed SBFI platform for detection of PKA activity was investigated by fluorescence imaging of single Dy-MBs in the presence of varying concentrations of PKA. Individual single Dy-MBs (80 ± 5 μm) are easily manipulated with a Narishige micromanipulator system. A bright halo around the bead surface can be observed in the fluorescence images (Figure 4a; Supporting Information, Figure S5). The brightness of the Dy-MB increases gradually with increasing activity of PKA from 0.5 $\mu U\,\mu L^{-1}$ to 80 $\mu U\,\mu L^{-1}$. The results of Figure 4a indicate that as low as 0.5 $\mu U\,\mu L^{-1}$ of PKA can produce a clear fluorescence signal that can be clearly distinguished from that of blank control. To acquire the quantitative fluorescence signals of the Dy-MBs, a z-stack fluorescence scan is performed on each single microbead. In such a scanning mode, each microbead is divided into 10 slices along the z-direction for laser scanning, and then the integrated fluorescence intensities of these slices are counted together for quantitative evaluation of PKA activities. The integrated fluorescence intensity (FI) of the microbead is linearly proportional to the PKA activity in the range from 0.5 ~ 4 $\mu U\,\mu L^{-1}$, and the calibration equation is $FI = 1.5 \times 10^6\ C_{PKA}\ (\mu U/\mu L) + 6.6 \times 10^4$ ($R = 0.9999$; Figure 4b). Higher concentrations of PKA can be detected at lower PMT voltages (Supporting Information, Figure S6). The detection limit of PKA is calculated to be 0.12 $\mu U\,\mu L^{-1}$ ($3\sigma, n = 11$), which is the lowest value known thus far because the detection limits of most of the existing PKA assays generally fall into the range of 10 ~ 500 $\mu U\,\mu L^{-1}$ (Supporting Information, Table S1). The performance of the Dy-MB-based SBFI system has been compared with those by using Zr^{4+}-functionalized microbead (Zr-MB) and TiO_2-coated microbead (Ti-MB). The lowest PKA activities that can be detected are ~8 $\mu U\,\mu L^{-1}$ and 20 $\mu U\,\mu L^{-1}$ by using the single Zr-MB and Ti-MB, respectively (Supporting Information, Figure S7). These results clearly suggest that Dy^{3+} exhibits the superior ability for recognizing phosphopeptides compared to the conventionally used TiO_2 and Zr^{4+}.

Owing to its ultrahigh sensitivity, the SBFI system was further examined for the direct detection of PKA activity in single MCF-7 cells. Forskolin/IBMX stimulation can increase the intracellular activity of PKA.[6k,10] In this study, both the forskolin/IBMX-stimulated and unstimulated MCF-7 single cell lysates were evaluated by the proposed SBFI system (Figure 5). No fluorescence signal was observed for the blank

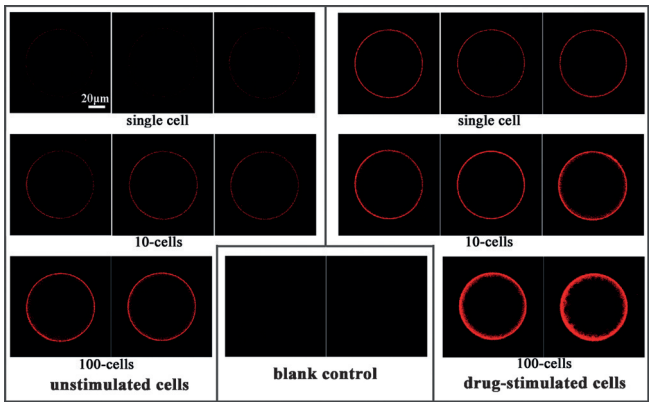

Figure 5. Fluorescence imaging results of the SBFI system for the direct detection of PKA activity in both forskolin/IBMX-stimulated (right panel) and unstimulated (left panel) cell samples containing single, 10, and 100 cells, respectively. PMT HV = 650 V.

control samples (containing lysis buffer only). As for the single cell samples unstimulated by forskolin/IBMX, relatively weak fluorescence on the Dy-MBs could be detected, which can be unequivocally distinguished from the blank control. In contrast, the forskolin/IBMX-treated single cell samples all produce intense fluorescence responses on the Dy-MBs that can be observed by the naked eye. Furthermore, we compared the results of the SBFI system by using single cell, 10 cells, and 100 cells for both the unstimulated cells and drug-stimulated cells. There is a clear trend indicating that the total PKA activity increases with the number of cells. All of these results show conclusively that the proposed SBFI strategy can measure changes in cellular kinase activities in response to stimuli at the single cell level.

In conclusion, towards the goal of single cell protein kinase analysis, we have first identified Dy^{3+} as the most prominent phospho-affinity element from the various RE ions tested. Then a single microbead, rather than numerous beads in conventional bioassays, is decorated with the selected Dy^{3+} and used as the ultimate assay unit to specifically enrich kinase-induced fluorescent phosphopeptides. By integrating the distinct advantages of Dy^{3+} for its highly strong and specific recognition ability towards kinase-induced phosphopeptides, and the highly-concentrated fluorescence accumulation effect on only one single microbead, an ultrasensitive SBFI strategy was developed. The activity of PKA can be detected and quantified, even in individual cells with the highest sensitivity known thus far. Owing to its high sensitivity, this newly proposed SBFI platform provides the potential to evaluate PK activities as well as the cellular signal transducing states of individual cells that exhibit a characteristic of interest, which may help our understanding of kinase-related disease initiation, progression, and therapeutic responses at the single-cell level.

Acknowledgements

This work was supported by the National Natural Science Foundation of China (21335005, 21472120, 21575086), the Natural Science Basic Research Plan of Shaanxi Province (2015KJXX-22), the Fundamental Research Funds for the Central Universities (GK201501003, GK201303003), the 111 Project (B14041) and Program for Innovative Research Team in Shaanxi Province (2014KCT-28).

Keywords: fluorescence imaging · kinases · rare earths · single cells · single microbeads

How to cite: *Angew. Chem. Int. Ed.* **2015**, *54*, 15186–15190
Angew. Chem. **2015**, *127*, 15401–15405

[1] a) J. Schlessinger, *Cell* **2000**, *103*, 211–225; b) J. A. Adams, *Chem. Rev.* **2001**, *101*, 2271–2290; c) G. Manning, D. B. Whyte, R. Martinez, T. Hunter, S. Sudarsanam, *Science* **2002**, *298*, 1912–1934.

[2] a) J. Brognard, T. Hunter, *Curr. Opin. Genet. Dev.* **2011**, *21*, 4–11; b) A. Salminen, K. Kaarniranta, A. Haapasalo, H. Soininen, M. Hiltunen, *J. Neurochem.* **2011**, *118*, 460–474; c) P. Blume-Jensen, T. Hunter, *Nature* **2001**, *411*, 355–365.

[3] a) J. Zhang, P. L. Yang, N. S. Gray, *Nat. Rev. Cancer* **2009**, *9*, 28–39; b) J. Dancey, E. A. Sausville, *Nat. Rev. Drug Discovery* **2003**, *2*, 296–313.

[4] a) T. Reya, S. J. Morrison, M. F. Clarke, I. L. Weissman, *Nature* **2001**, *414*, 105–111; b) A. A. Cohen, N. Geva-Zatorsky, E. Eden, M. Frenkel-Morgenstern, I. Issaeva, A. Sigal, R. Milo, C. Cohen-Saidon, Y. Liron, Z. Kam, L. Cohen, T. Danon, N. Perzov, U. Alon, *Science* **2008**, *322*, 1511–1516; c) D. Wang, S. Bodovitz, *Trends Biotechnol.* **2010**, *28*, 281–290.

[5] a) G. D. Meredith, C. E. Sims, J. S. Soughayer, N. L. Allbritton, *Nat. Biotechnol.* **2000**, *18*, 309–312; b) S. Mehta, J. Zhang, *Annu. Rev. Biochem.* **2011**, *80*, 375–401; c) L. F. Cheow, A. Sarkar, S. Kolitz, D. Lauffenburger, J. Han, *Anal. Chem.* **2014**, *86*, 7455–7462; d) A. Sarkar, S. Kolitz, D. A. Lauffenburger, J. Han, *Nat. Commun.* **2014**, *5*, 3421.

[6] a) Z. Wang, R. Lévy, D. G. Fernig, M. Brust, *J. Am. Chem. Soc.* **2006**, *128*, 2214–2215; b) Y. P. Kim, E. Oh, Y. H. Oh, D. W. Moon, T. G. Lee, H. S. Kim, *Angew. Chem. Int. Ed.* **2007**, *46*, 6816–6819; *Angew. Chem.* **2007**, *119*, 6940–6943; c) O. I. Wilner, C. Guidotti, A. Wieckowska, R. Gill, I. Willner, *Chem. Eur. J.* **2008**, *14*, 7774–7781; d) R. Freeman, T. Finder, R. Gill, I. Willner, *Nano Lett.* **2010**, *10*, 2192–2196; e) J. E. Ghadiali, B. E. Cohen, M. M. Stevens, *ACS Nano* **2010**, *4*, 4915–4919; f) S. Gupta, H. Andresen, J. E. Ghadiali, M. M. Stevens, *Small* **2010**, *6*, 1509–1513; g) H. W. Rhee, S. H. Lee, I. S. Shin, S. J. Choi, H. H. Park, K. Han, T. H. Park, J. I. Hong, *Angew. Chem. Int. Ed.* **2010**, *49*, 4919–4923; *Angew. Chem.* **2010**, *122*, 5039–5043; h) S. Martic, M. Gabriel, J. P. Turowec, D. W. Litchfield, H. B. Kraatz, *J. Am. Chem. Soc.* **2012**, *134*, 17036–17045; i) J. Bai, Y. Zhao, Z. Wang, C. Liu, Y. Wang, Z. Li, *Anal. Chem.* **2013**, *85*, 4813–4821; j) W. Ren, C. Liu, S. Lian, Z. Li, *Anal. Chem.* **2013**, *85*, 10956–10961; k) J. Zhou, X. Xu, W. Liu, X. Liu, Z. Nie, M. Qing, L. Nie, S. Yao, *Anal. Chem.* **2013**, *85*, 5746–5754; l) N. P. Oien, L. T. Nguyen, F. E. Jernigan, M. A. Priestman, D. S. Lawrence, *Angew. Chem. Int. Ed.* **2014**, *53*, 3975–3978; *Angew. Chem.* **2014**, *126*, 4056–4059; m) A. M. Lipchik, M. Perez, S. Bolton, V. Dumrongprechachan, S. B. Ouellette, W. Cui, L. L. Parker, *J. Am. Chem. Soc.* **2015**, *137*, 2484–2494; n) X. Liu, Y. Li, X. Xu, P. Li, Z. Nie, Y. Huang, S. Yao, *TrAC Trends Anal. Chem.* **2014**, *58*, 40–53; o) J. A. González-Vera, *Chem. Soc. Rev.* **2012**, *41*, 1652–1664.

[7] a) W. Ren, H. Liu, W. Yang, Y. Fan, L. Yang, Y. Wang, C. Liu, Z. Li, *Biosens. Bioelectron.* **2013**, *49*, 380–386; b) Y. Zhang, C. Liu, S. Sun, Y. Tang, Z. Li, *Chem. Commun.* **2015**, *51*, 5832–5835; c) P. Tan, C. Lei, X. Liu, M. Qing, Z. Nie, M. Guo, Y. Huang, S. Yao, *Anal. Chim. Acta* **2013**, *780*, 89–94.

[8] a) J. Ji, H. Yang, Y. Liu, H. Chen, J. Kong, B. Liu, *Chem. Commun.* **2009**, 1508 – 1510; b) X. Xu, Z. Nie, J. Chen, Y. Fu, W. Li, Q. Shen, S. Yao, *Chem. Commun.* **2009**, 6946 – 6948; c) F. Rininsland, W. Xia, S. Wittenburg, X. Shi, C. Stankewicz, K. Achyuthan, D. McBranch, D. Whitten, *Proc. Natl. Acad. Sci. USA* **2004**, *101*, 15295 – 15300.

[9] a) M. R. Mirza, M. Rainer, C. B. Messner, Y. Guzel, D. Schemeth, T. Stasyk, M. I. Choudhary, L. A. Huber, B. M. Rode, G. K. Bonn, *Analyst* **2013**, *138*, 2995 – 3004; b) A. Vilasi, I. Fiume, P. Pace, M. Rossi, G. Pocsfalvi, *J. Mass Spectrom.* **2013**, *48*, 1188 – 1198.

[10] C. Liu, L. Chang, H. Wang, J. Bai, W. Ren, Z. Li, *Anal. Chem.* **2014**, *86*, 6095 – 6102.

[11] F. Jabeen, M. Najam-ul-Haq, M. Rainer, Y. Güzel, C. W. Huck, G. K. Bonn, *Anal. Chem.* **2015**, *87*, 4726 – 4732.

[12] S. Lipstman, S. Muniappan, S. George, I. Goldberg, *Dalton Trans.* **2007**, 3273 – 3281.

[13] a) D. Costa, H. D. Burrows, M. da Graça Miguel, *Langmuir* **2005**, *21*, 10492 – 10496; b) L. L. Li, P. Wu, K. Hwang, Y. Lu, *J. Am. Chem. Soc.* **2013**, *135*, 2411 – 2414; c) L. L. Li, Y. Lu, *J. Am. Chem. Soc.* **2015**, *137*, 5272 – 5275.

Received: August 13, 2015
Revised: September 13, 2015
Published online: October 20, 2015

